

Sweet taste of heavy water

Natalie Ben Abu^{1,2,5}, Philip E. Mason^{3,5}, Hadar Klein^{1,2}, Nitzan Dubovski^{1,2}, Yaron Ben Shoshan-Galeczki^{1,2}, Einav Malach^{1,2}, Veronika Pražienková³, Lenka Maletínská³, Carmelo Tempa³, Victor Cruces Chamorro³, Josef Cvačka³, Maik Behrens⁴, Masha Y. Niv^{1,2}✉ & Pavel Jungwirth³✉

Hydrogen to deuterium isotopic substitution has only a minor effect on physical and chemical properties of water and, as such, is not supposed to influence its neutral taste. Here we conclusively demonstrate that humans are, nevertheless, able to distinguish D₂O from H₂O by taste. Indeed, highly purified heavy water has a distinctly sweeter taste than same-purity normal water and can add to perceived sweetness of sweeteners. In contrast, mice do not prefer D₂O over H₂O, indicating that they are not likely to perceive heavy water as sweet. HEK 293T cells transfected with the TAS1R2/TAS1R3 heterodimer and chimeric G-proteins are activated by D₂O but not by H₂O. Lactisole, which is a known sweetness inhibitor acting via the TAS1R3 monomer of the TAS1R2/TAS1R3, suppresses the sweetness of D₂O in human sensory tests, as well as the calcium release elicited by D₂O in sweet taste receptor-expressing cells. The present multifaceted experimental study, complemented by homology modelling and molecular dynamics simulations, resolves a long-standing controversy about the taste of heavy water, shows that its sweet taste is mediated by the human TAS1R2/TAS1R3 taste receptor, and opens way to future studies of the detailed mechanism of action.

¹The Institute of Biochemistry, Food Science and Nutrition, The Robert H Smith Faculty of Agriculture, Food and Environment, The Hebrew University of Jerusalem, Rehovot, Israel. ²The Fritz Haber Center for Molecular Dynamics, The Hebrew University of Jerusalem, Jerusalem, Israel. ³Institute of Organic Chemistry and Biochemistry, Czech Academy of Sciences, Prague 6, Czech Republic. ⁴Leibniz-Institute for Food Systems Biology at the Technical University of Munich, Freising, Germany. ⁵These authors contributed equally: Natalie Ben Abu, Philip E. Mason. ✉email: masha.niv@mail.huji.ac.il; pavel.jungwirth@uochb.cas.cz

Heavy water, D₂O, has fascinated researchers since the discovery of deuterium by Urey in 1931^{1,2}. The most notable difference in physical properties between D₂O and H₂O is the roughly 10% higher density of the former liquid, which is mostly a trivial consequence of deuterium being about twice as heavy as hydrogen. A more subtle effect of deuteration is the formation of slightly stronger hydrogen (or deuterium) bonds in D₂O as compared to H₂O^{3,4}. This results in a small increase of the freezing and boiling points by 3.8 °C and 1.4 °C, respectively, and in a slight increase of 0.44 in pH (or pD) of pure water upon deuteration⁵. In comparison, a mere dissolution of atmospheric CO₂ and subsequent formation of dilute carbonic acid in open containers has a significantly stronger influence on the pH of water, changing it by more than one unit⁶.

Biological effects are observable for high doses of D₂O. While bacteria or yeasts can function in practically pure D₂O, albeit with somewhat hindered growth rate^{7–9}, for higher organisms damaging effects on cell division and general metabolism occur at around 25% deuteration, with lethal conditions for plants and animals typically occurring at ~40–50% deuteration of the body water^{2,10,11}. Small levels of deuteration are, nevertheless, harmless. This is understandable given the fact that about 1 in every 6400 hydrogens in nature is found in its stable isotope form of deuterium¹². Oral doses of several milliliters of D₂O are safe for humans¹³ and are used in the isotopic form D₂¹⁸O for metabolic measurements in clinical praxis (known as “doubly labeled water” technique)¹⁴. Probably the best-established effect of D₂O is the increase of the circadian oscillation length upon its administration to both animals and plants. This has been attributed to a general slowdown of metabolism upon deuteration, although the exact mechanism of this effect is unknown^{15,16}.

A long-standing unresolved puzzle concerns the taste of heavy water. There is anecdotal evidence from the 1930s that the taste of pure D₂O is distinct from the neutral one of pure H₂O, being described mostly as “sweet”¹⁷. However, Urey and Failla addressed this question in 1935 concluding authoritatively that upon tasting “neither of us could detect the slightest difference between the taste of ordinary distilled water and the taste of pure heavy water”¹⁸. This had, with a rare exception¹⁹, an inhibitive effect on further human studies, with research concerning effects of D₂O focusing primarily on animal or cell models. Experiments in animals indicated that rats developed aversion toward D₂O when deuteration of their body water reached harmful levels, but there is conflicting evidence regarding their ability to taste heavy water or use other cues to avoid it^{20,21}.

Within the last two decades, the heterodimer of the taste receptor of the TAS1Rs type of G protein-coupled receptors (GPCRs), denoted as TAS1R2/TAS1R3, was established as the main receptor for sweet taste²². The human TAS1R2/TAS1R3 heterodimer recognizes diverse natural and synthetic sweeteners²³. The binding sites of the different types of sweeteners include an orthosteric site (a sugar-binding site in the extracellular Venus flytrap domain of TAS1R2) and several allosteric sites, including sites in the extracellular regions of the TAS1R2 and TAS1R3 subunits and in the transmembrane domain of TAS1R3^{24,25} (Fig. 1). Additional pathways for sweet taste recognition have also been suggested, involving glucose transporters and ATP-gated K⁺ channel^{26,27}.

Interestingly, not all artificial sweeteners are recognized by rodents²⁸. Differences in human and rodent responses to tastants, as well as sweetness inhibitors such as lactisole, have been useful for delineating the molecular recognition of sweet compounds—using human-mouse chimeric receptors, it was shown that the transmembrane domain (TMD) of human TAS1R3 is required for the activating effects of cyclamate²⁹ and for the inhibitory effect of lactisole³⁰.

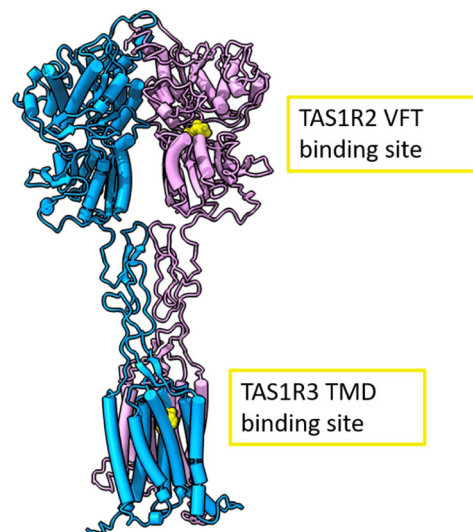


Fig. 1 Full human sweet taste TAS1R2/TAS1R3 receptor model with the TAS1R2 monomer colored in pink and the TAS1R3 monomer in cyan.

Binding sites are represented in yellow. The full receptor heterodimer was prepared with the I-Tasser web server⁵¹ based on multiple experimental structures (i.e., 6N51, 5X2M, and 5K5S). The binding site of TAS1R2 is based on coordinates of docked D-glucose to a Venus flytrap (VFT)⁵⁹ (modeling based on template PDB ID: 5X2M, docking performed with Schrödinger Maestro 2019-1, Glide XP), and the TAS1R3-binding site is based on a lactisole molecule docked to the TAS1R3 TMD model (template PDB IDs: 4OR2 and 4O09, Schrödinger Maestro 2018-2, Glide SP). The figure was made using ChimeraX (version 0.93)⁶⁰.

A combination of TAS1R3 with another member of the TAS1R family, TAS1R1, results in a dimer that mediates umami taste, elicited by molecules such as glutamate or, in case of the rodent umami receptor, other L-amino acids³¹. Bitter taste is mediated by the taste 2 receptor (TAS2R) gene family³², a branch of Family A GPCRs²⁴. The human genome has 25 TAS2R subtypes and over a thousand of bitter compounds are currently known³³, with numerous additional bitter tastants predicted³⁴.

In this study, we systematically address the question of sweet taste of heavy water by a combination of sensory experiments in humans, behavioral experiments in mice, tests on sweet taste receptor-transfected cell lines, and computational modeling including molecular dynamics (MD) simulations. This combined approach consistently leads to the conclusion that the sweet taste of pure D₂O is a real effect for human subjects due to activation of the TAS1R2/TAS1R3 sweet taste receptor. While present simulations show, in accord with previous experiments³⁵, that proteins are systematically slightly more rigid and compact in D₂O than in H₂O, the specific molecular mechanism of the heavy water effect on the TAS1R2/TAS1R3 receptor remains to be established.

Results and discussion

Water purity. We have paid great attention to the purity of the water samples, further degassing and redistilling under vacuum the purest commercially available D₂O and H₂O. The lack of non-negligible amounts of organic impurities was subsequently confirmed by gas chromatography with mass spectrometry analysis and by experiments with water samples at different levels of purification, see Supplementary Information (SI), Figures S1 and S2. This is extremely important—note in this context that “the vibrational theory of olfaction”, which suggested distinct perception of deuterium isotopes of odorants due to difference in

their vibrational spectra³⁶, has been refuted with some of the observed effects turning out to be due to impurities^{37,38}.

Experiments with a human sensory panel. A human sensory panel was employed to study the D₂O taste. Triangle tests based on two samples of H₂O and one sample of D₂O (or vice versa), with random success rate of one-third, were presented to the panelists in a randomized order. Panelists were asked to pick the odd sample out—to smell only, to taste only (with a nose clips), or to taste with open nose. Our results show that humans perceive D₂O as being clearly distinguishable from H₂O based on its taste: In open nose taste test 22 out of 28 participants identified the odd sample correctly ($p = 0.001$), and in taste only test 14 out of 26 identified the odd sample correctly ($p = 0.03$). However, in smell-only triangle test, only 9 out of 25 panelists chose the odd sample correctly ($p > 0.05$). Data are summarized in Figure S3 in SI.

Next, the perceived sweetness of D₂O in increasing proportion to H₂O was reported using a 9-point scale, labeled also with verbal descriptions of perceived intensity (1 = no sensation, 3 = slight, 5 = moderate, 7 = very much, 9 = extreme sensation). Sweetness was shown to increase in a D₂O-dose-dependent manner, reaching average 3.3 ± 0.4 sweetness (“slight” sweetness) (Fig. 2a). The perceived sweetness of low concentrations of caloric D-glucose (Fig. 2b), sucrose (Fig. 2c), and an artificial sweetener cyclamate (Fig. 2d) was tested when dissolved in H₂O or in D₂O, in order to check whether the slight sweetness of D₂O adds on top of slight sweetness of known sweeteners. As expected³⁹, D-glucose was perceived as less sweet compared to sucrose at the same concentration (Fig. 2b and c). D₂O added to the perceived sweetness of all tested concentrations of D-glucose and cyclamate (see Figure S4 in the SI for cyclamate results excluding two outliers). The sweetness of the two lowest concentrations of sucrose was significantly higher when dissolved in D₂O compared to H₂O.

We then checked whether the stand-alone and additive effect of D₂O is sweetness-specific or general, whereby D₂O might elicit other tastes, or add to their intensity. Savory (umami) taste of monosodium glutamate (MSG) and bitter taste of quinine, which are also taste modalities mediated by GPCR receptors expressed in taste cells, were tested in regular and in heavy water. The intensity of savory taste of MSG in D₂O did not differ from that in H₂O (Fig. 2e), while the perceived bitterness of quinine was in fact slightly reduced in D₂O compared to quinine in H₂O (Fig. 2f). This is in agreement with the known effect of sweeteners as maskers of bitter taste, that may be due to both local interactions and sensory integration effects^{40–42}. Thus, we have ascertained that D₂O is sweet and adds to the sweetness of other sweet molecules, but not to the intensity of other GPCR-mediated taste modalities.

Experiments with mice. Next, we addressed the question whether the sweetness of D₂O is perceived also by rodents. Lean mice of the C57BL/6J strain were drinking pure H₂O, D₂O, or a 43 mmol/l H₂O sucrose solution for 16 h during a night period. Namely, each of the three groups of mice had a choice from two bottles containing (i) H₂O and D₂O, (ii) H₂O and sucrose solution, or (iii) H₂O and H₂O (as a control). The food intake was unaffected in all groups (see SI, Figure S5 and Table S1).

The results of the drinking experiments are presented in Fig. 3a–c, with a snapshot of the experimental setup shown in Fig. 3d. In cages where mice were offered both normal water and heavy water (Fig. 3a) consumption of D₂O was within statistical error the same as that of H₂O. Previous reports have shown that on longer timescales than those reported here mice learned to avoid D₂O, as it is poisonous to them in larger quantities¹⁰. It is

not clear what is the cue that enables the avoidance learning, but it is evident that the early response to D₂O is not attractive, suggesting that it is not eliciting sweet taste in mice.

By contrast, mice exhibit a strong preference for sucrose solution over H₂O. Indeed, the consumed volume was significantly increased in line with the predilection of mice for sucrose solutions (Fig. 3b). The amount of H₂O consumed by the control group from either of the two bottles, both containing H₂O, is depicted in Fig. 3c. Overall, the data shows that in all three experiments mice consumed comparable amounts of H₂O and D₂O, with significant increase of consumption of the sucrose solution.

Assessing involvement of TAS1R2/TAS1R3 receptor using human sensory panel. The chemical dissimilarity of D₂O from sugars and other sweeteners raises the question whether the effect we observed in human subjects is mediated by TAS1R2/TAS1R3, which is the major receptor for sweet taste²². This was first explored by combining water samples with lactisole as an established TAS1R2/TAS1R3 inhibitor³⁰. Using the two-alternative forced-choice (2AFC) method, in which the participant must choose between two samples, 18 out of 25 panelists chose pure D₂O as sweeter than D₂O + 0.9 mM lactisole solution ($p < 0.05$, Fig. 4a). In an additional experiment, the sweetness of pure D₂O was scored significantly higher than that of D₂O + 0.9 mM lactisole solution ($p = 0.0003$), while the same amount of lactisole had no effect on the perception of sweetness of H₂O that served as control (Fig. 4b). These results suggest that D₂O elicits sweetness via the TAS1R2/TAS1R3 sweet taste receptor.

Cell-based experiments for establishing the role of TAS1R2/TAS1R3. To confirm the involvement of the sweet taste receptor TAS1R2/TAS1R3 in D₂O signaling we performed functional calcium mobilization assays using HEK 293 FlpIn T-Rex cells heterologously expressing both required TAS1R subunits as well as the chimeric G protein Ga15Gi3^{43,44}. As seen in Fig. 5a, D₂O at 1.85 M and 5.84 M concentrations in H₂O (3.3% and 10.4%, respectively) elicited robust responses in TAS1R2/TAS1R3 expressing cells. The strong reduction or absence of D₂O-elicited fluorescence response in the presence of lactisole confirmed the dependence on TAS1R2/TAS1R3. The inhibitory effect of lactisole on D₂O-activation of the human sweet taste receptor was confirmed using an IP1 assay^{45,46}, while lactisole exposure had no effect on cells treated with pure H₂O water, as expected (Fig. 5c). As a control, 960 mM D-glucose elicited increase in IP1 levels in TAS1R2/TAS1R3 expressing cell, which was inhibited in the presence of lactisole.

We further used an IP1 assay^{45,46} on non-transfected HEK 293T cells, where we observed that dose-dependent curves of carbachol—an agonist of the endogenous muscarinic receptor 3 (M3)⁴⁷—did not show any difference between H₂O and D₂O-based media (Fig. 6a) and that cell medium that had either 10% or 100% D₂O, did not activate basal IP1 accumulation (Fig. 6b). Next, TAS1R2/TAS1R3 receptor along with the chimeric Ga16gust44 subunit^{44,48} were transiently expressed, and the functionality was illustrated by dose-dependent response to D-glucose (Fig. 6c). Finally, and in agreement with calcium imaging, we found that 10% D₂O activated these cells. Activation by 100% D₂O was even more pronounced (Fig. 6d).

Molecular modeling. The cellular response results further support the hypothesis that the sweet taste of D₂O is mediated via the TAS1R2/TAS1R3 receptor. Various mechanisms governing this effect can be envisioned. As a potential suspect, we focus on a direct effect on the sweet taste receptor, narrowing on the

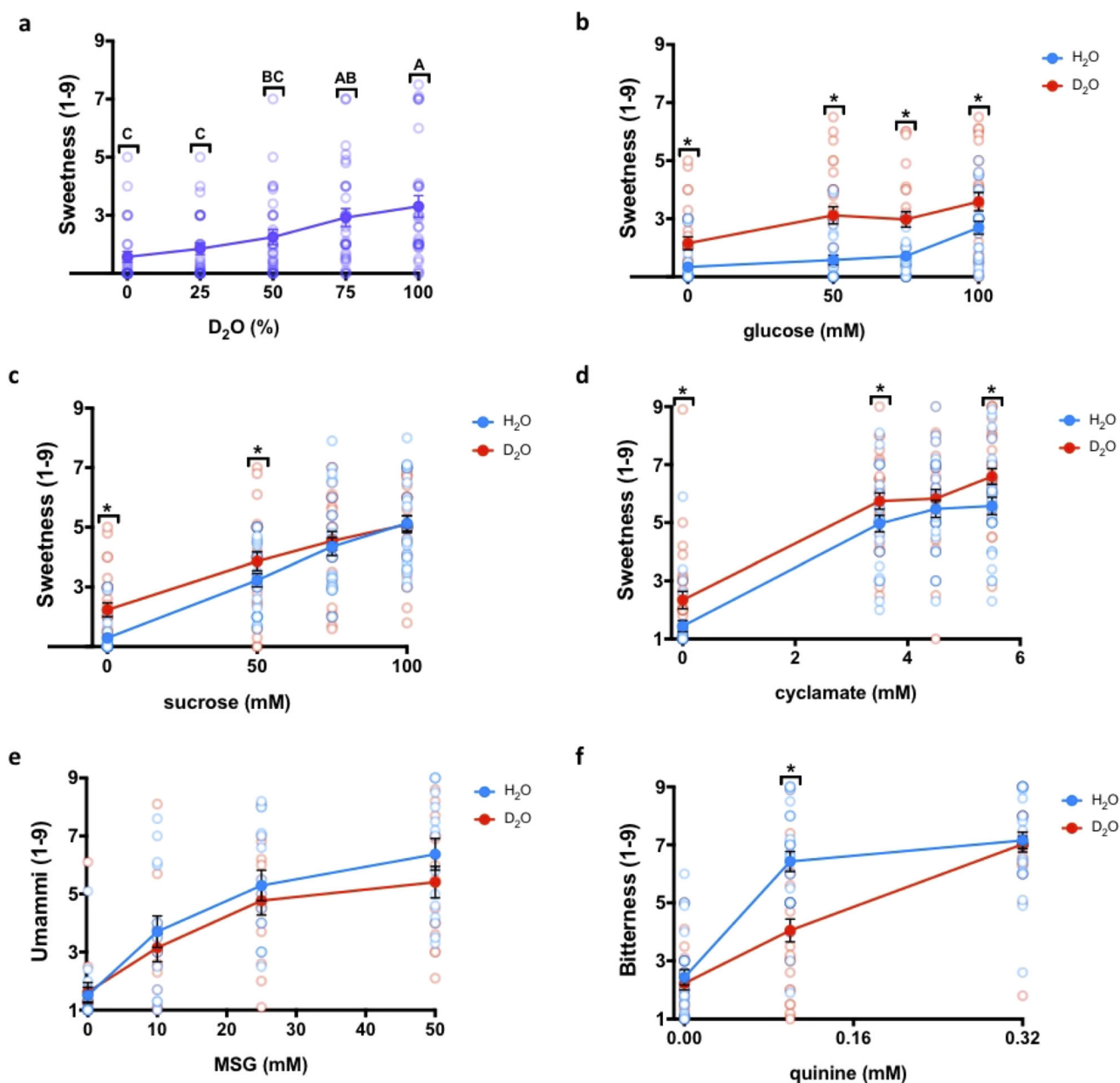


Fig. 2 D₂O sweetness and its effect on different tastants. **a** Sweetness of D₂O mixed at increasing ratios with H₂O. Treatments not connected by the same letters are significantly different ($p < 0.05$ in Tukey Kramer test). **b-f** The effect of D₂O (red) compared to H₂O (blue) on glucose (**b**), sucrose (**c**), cyclamate (**d**), quinine (**e**), and MSG (**f**) taste-specific intensity. Asterisks indicate a significant ($p < 0.05$) difference between water types using the two-way analysis of variance (ANOVA) with a preplanned comparison t -test. All data are presented as the mean \pm the Standard Error of Measurement (SEM); $n = 15-30$ (4-12 males). The y axis shows the response for individual modalities, while the x axis is labeled with different water samples. Scale for each modality is labeled as 1 = no sensation, 3 = slight, 5 = moderate, 7 = very much, and 9 = extreme sensation.

TAS1R3 TMD (see Fig. 1), as it is already known to be a modulation site with functional differences between humans and rodents^{23,29,30}. Furthermore, water-binding sites were discovered at the TMD of many GPCRs^{49,50}, suggesting a potential target for D₂O binding. We modeled the human TAS1R3 TMD using the I-TASSER server⁵¹. Positions of H₂O molecules were compared among mGluR5 structures (PDB: 4OO9, 5CGC, and 5CGD) and two conserved positions were found. The H₂O molecules in these two positions were merged with the TAS1R3 model and minimized (Fig. 7a). The water mapping protocol from OpenEye⁵² enables mapping of water positions based on the energetics of water, and ~ 40 water molecules were predicted in the binding site using this protocol (Fig. 7a). Water densities of H₂O and D₂O in

the TMD of the TAS1R2/TAS1R3 receptor were calculated from MD simulations as described below. Overall, all three methods suggest the possibility for at least some internal molecules (trapped in the TMD bundle) in addition to water that surrounds the extracellular and intracellular loops (Fig. 7a).

Next, we carried out microsecond MD simulations of the TMD embedded in a phosphatidylcholine (POPC) bilayer in either H₂O or D₂O (for details including our model of D₂O effectively including nuclear quantum effects, see SI, Tables S2-S4). Note that water molecules enter the TMD domain and cluster at positions that partially overlap with the modeled water positions, see Fig. 7a. More precisely, H₂O and D₂O have mutually slightly shifted densities inside the protein cavity, with H₂O overlapping

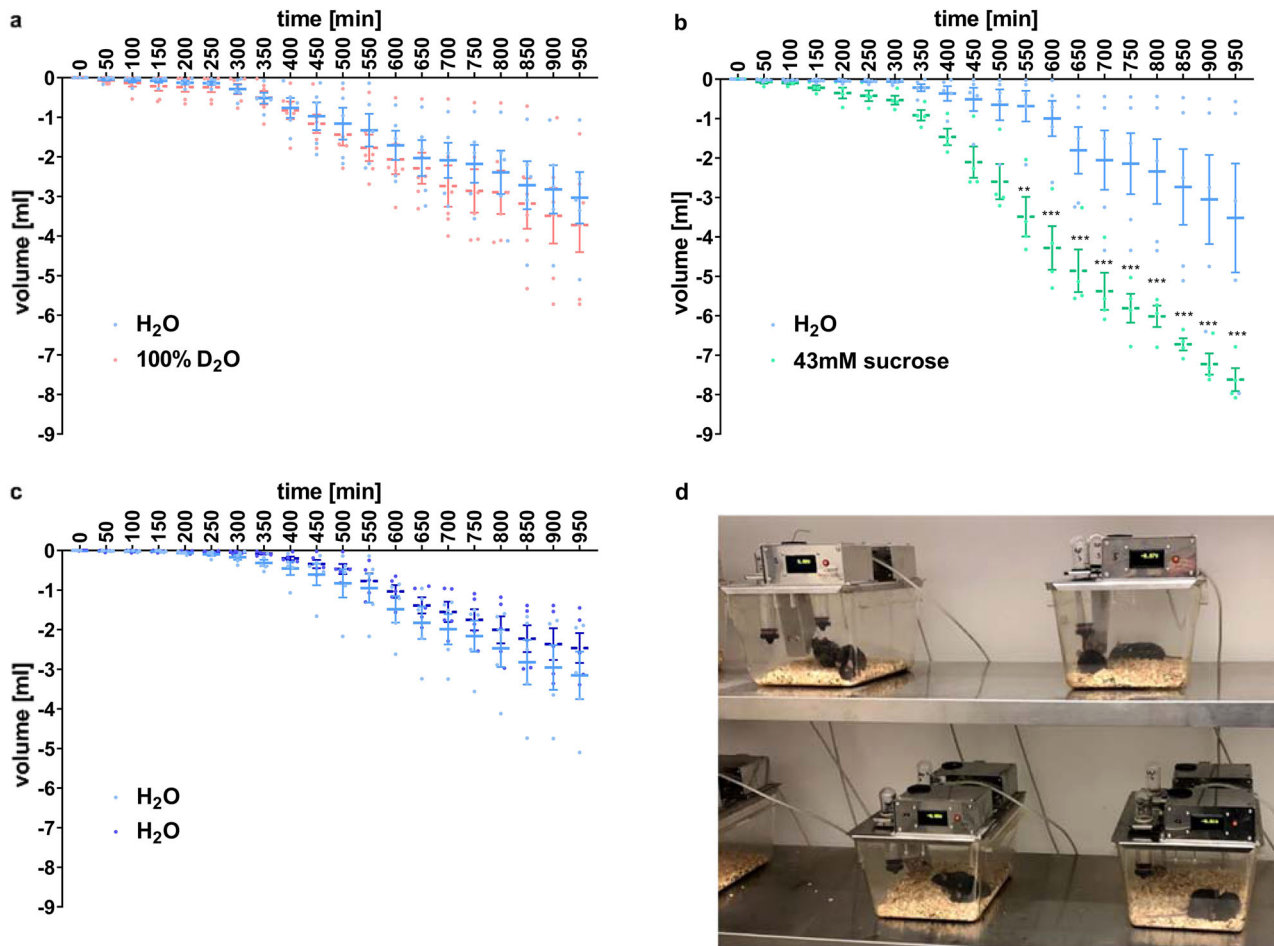


Fig. 3 Time-resolved volumes of water consumption by mice. **a** Volume consumption of D₂O is not different from that of H₂O (*n* = 12). **b** Mice show strong preference to sucrose solution (*n* = 10). Significance is ***p* < 0.01, ****p* < 0.001. **c** Volume consumption of the control group drinking H₂O only (*n* = 12). **d** Snapshot of the automatic drinking monitoring system. Mice were placed in groups of two in individual cages. Data are presented as the mean ± standard error of the mean (SEM). Statistical analysis was performed using two-way ANOVA with a Bonferroni’s multiple comparisons test.

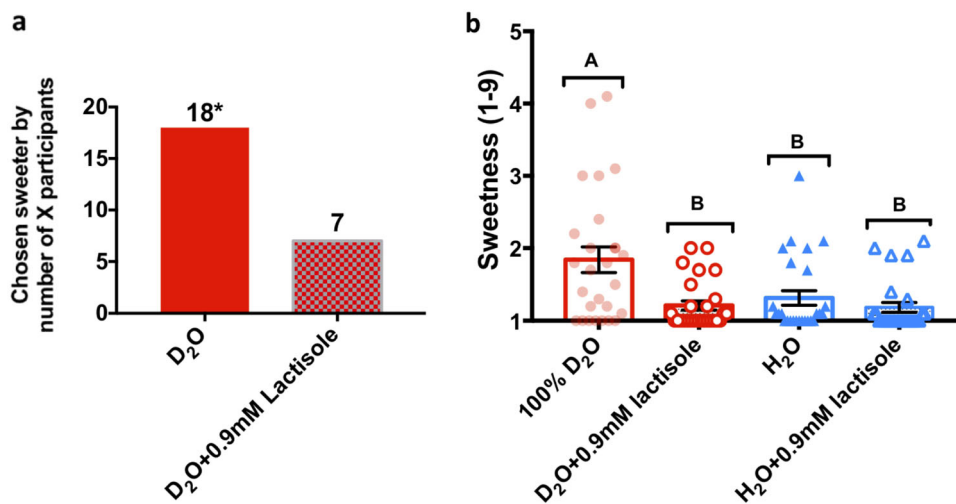


Fig. 4 Lactisole reduces sweetness of D₂O. **a** 2AFC test. Pure D₂O was chosen to be sweeter (*p* < 0.05) than the sample with lactisole by 18 participants (*n* = 25; 11 males). **b** Effect of 0.9 mM lactisole on sweetness intensity using the 9-point scale. Data are presented as the mean ± SEM. The y axis shows the response for sweetness on a 9-point scale, while the x axis is labeled with different water samples. Statistical analysis was performed using ANOVA with a Tukey Kramer test (*n* = 27; 9 males); treatments not connected by the same letters are significantly different (*p* < 0.05). Scale for sweetness is labeled as 1 = no sensation, 3 = slight, 5 = moderate, 7 = very much, and 9 = extreme sensation.

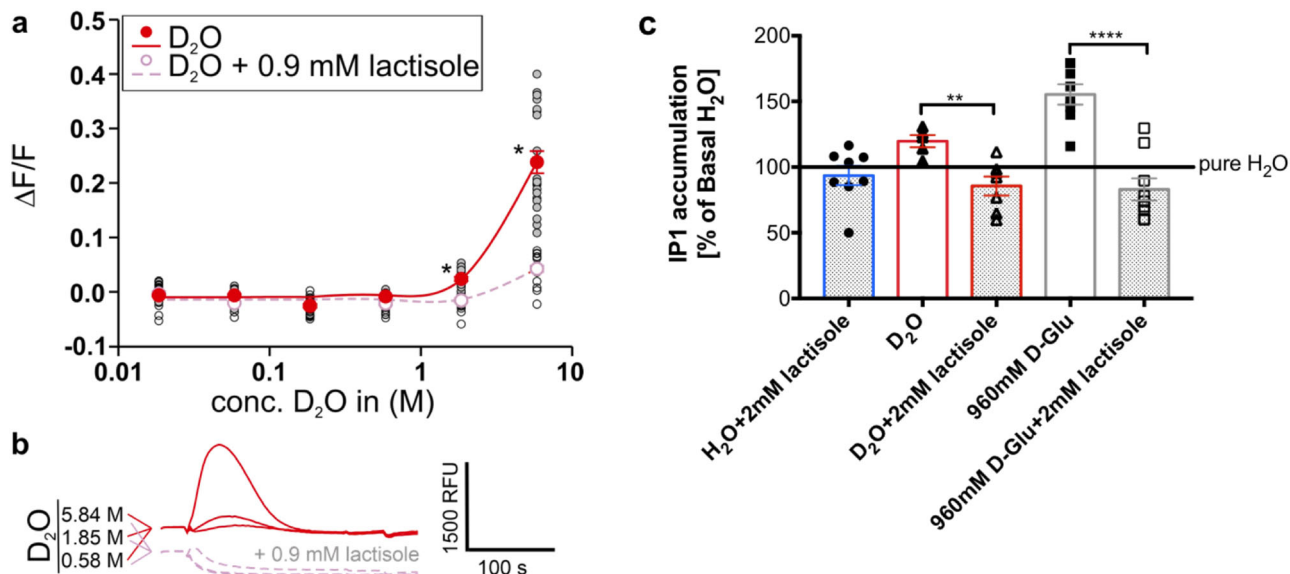


Fig. 5 D₂O-activation of the human sweet taste receptor. **a** Dose-response relationship of cells expressing the human sweet taste receptor and treated with different concentrations of D₂O (filled red circles, red line). Cells treated with lactisole served as negative controls (open pink circles, pink line). y axis, relative changes in fluorescence upon stimulus application ($\Delta F/F$). x axis, logarithmically scaled molar D₂O-concentrations. Asterisks indicate fluorescence changes above baseline significantly different from lactisole-treated controls ($p \leq 0.01$). **b** Raw fluorescence traces of D₂O-treated (red-traces, top) and D₂O + 0.9 mM lactisole-treated cells (pink-traces, bottom) stimulated with the indicated D₂O-concentrations. A scale bar indicating relative fluorescence (relative fluorescence units (RFU)) and experimental time (in seconds (s)) is included. **c** Lactisole inhibitory effect on D₂O-activation of the human sweet taste receptor using an IP1 assay. Cells treated with D-glucose served as positive controls. On y axis, relative changes in IP1 accumulation upon stimulus application are shown as % of basal-pure H₂O. x axis, different ligands, with and without lactisole. Asterisks indicate IP1 changes that are significantly different from lactisole-treated controls (** $p \leq 0.005$ and **** $p \leq 0.0001$) using *t*-test.

better than D₂O with the modeled water positions. Furthermore, MD simulations show clustered water molecules close to the lactisole binding site. These internal positions may have a differential effect between H₂O and D₂O, though differences between the averaged water densities are not very pronounced. Figure 7b shows the time evolution of the radius of gyration of the TMD domain, while Fig. 7c and d presents the root mean square fluctuations (RMSF) of individual residues of the proteins superimposed on its structure and plotted in a graph together with the mean value of RMSF. A small but significant difference is apparent in the behavior of the protein in H₂O vs D₂O. Namely, structural fluctuations of most residues (particularly those directly exposed to the aqueous environment) and of the protein as a whole are slightly attenuated in D₂O, in which environment the protein is also somewhat more compact than in H₂O (Fig. 7b). Additional simulations on other representative systems show that the rigidifying effect of heavy water is apparent also in small soluble proteins (see SI, Figs. S6–S8).

Summary and outlook. Sweet taste never ceases to surprise. Over a decade ago, water was shown to elicit sweet taste by rinsing away inhibitors of sweet taste receptors, both in human sensory experiments and in cell-based studies. This effect was explained in terms of a two-state model, where the receptor shifts to its activated state when released from inhibition by rinsing with water⁴³. Here, we have studied the taste of D₂O and H₂O per se, not related to washing away of sweet taste inhibitors. Using psychophysics protocols, we show that humans differentiate between D₂O and H₂O based on taste alone. Importantly, by employing gas chromatography/mass spectrometry analysis we demonstrate that the sweet taste of deuterated water is not due to impurities. Being only isotopically different from H₂O, in principle, D₂O should be indistinguishable from H₂O with regard to taste, namely it should have no taste of its own. Yet, we illustrate that

human subjects consistently perceive D₂O as being slightly sweet and significantly sweeter than H₂O. Furthermore, D₂O added to perceived sweetness of low concentrations of other sweeteners. In contrast, it did not elicit umami or bitter taste on its own, nor did it add to the umami taste perception of MSG. D₂O did not add to the bitterness of quinine, and reduced the perceived bitterness of 0.1 mM quinine, in agreement with the known effect of bitterness suppression by sweet molecules.

A further important finding is that lactisole, which is an established blocker of the TAS1R2/TAS1R3 sweet taste receptor that acts at the TAS1R3 transmembrane domain³⁰, suppresses both the sweet perception of D₂O in sensory tests, as well as the activation of TAS1R/TAS1R3 in calcium imaging and in IP1 cell-based assays. In support of these observations we have demonstrated that HEK 293T cells transfected with TAS1R2/TAS1R3 and Ga16gust44 chimera, but not the non-transfected cells, are activated by D₂O, as measured by IP1 accumulation compared to control values. Finally, taste experiments on mice show that these animals do not prefer D₂O over H₂O.

Our findings point to the human sweet taste receptor TAS1R2/TAS1R3 as being essential for sweetness of D₂O. Molecular dynamics simulations show, in agreement with experiment³⁵, that proteins in general are slightly more rigid and compact in D₂O than in H₂O. At a molecular level, this general behavior may be traced back to the slightly stronger hydrogen bonding in D₂O vs H₂O, which is due to a nuclear quantum effect, namely difference in zero-point energy^{3,4}. Biologically relevant situations where one may expect strong nuclear quantum effects as implications of H/D substitution directly involve proton or deuteron transfer⁹. Unless a yet unknown indirect mechanism is involved, this is not the case for the TAS1R2/TAS1R3 sweet taste receptor, thus the nuclear quantum effect is probably weak in the present case. Future studies should be able to elucidate the precise sites and mechanisms of action, as well as the reason why D₂O activates TAS1R2/TAS1R3

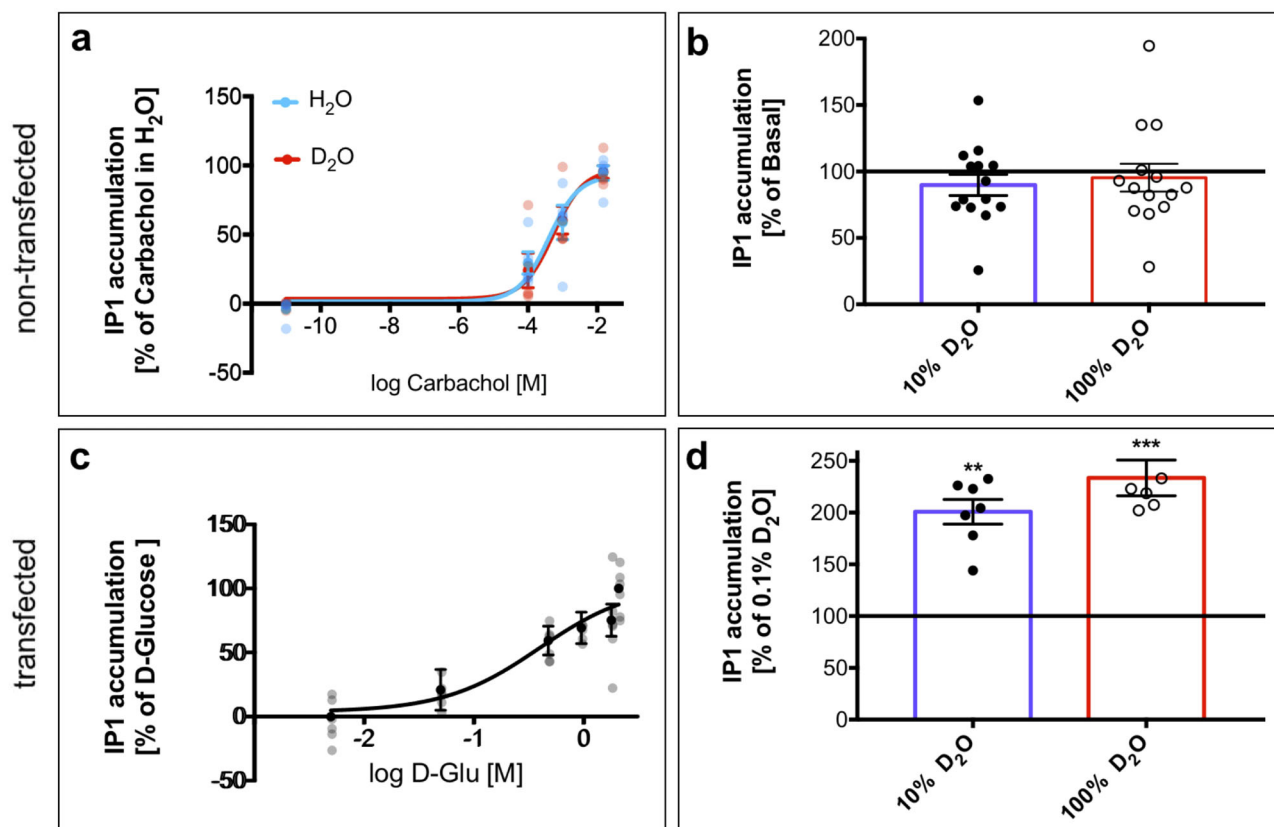


Fig. 6 IP1 accumulation in HEK 293T cells following exposure to different ligands dissolved in powder-based DMEM medium. **a** Non-transfected HEK 293T cells respond similarly to raising concentrations of carbachol dissolved in D₂O (red) as in H₂O (blue). **b** D₂O caused no elevation of IP1 levels in non-transfected HEK 293T cells. **c** HEK 293T cells transiently expressing TAS1R2/TAS1R3 respond positively to D-glucose. **d** Transfected HEK 293T cells are activated by D₂O. Values represent the mean ± SEM of at least three replicates. The horizontal black line represents the basal values of controls. Significant differences in IP1 values from control values are marked with ** $p \leq 0.005$ and *** $p \leq 0.0005$ using Dunnett's multiple comparisons test.

in particular, resulting in sweet (but not other) taste. To this end, site-directed mutagenesis as well as determination of the precise structure of the TAS1R2/TAS1R3 receptor will be of key importance.

The finding that deuterated water elicits sweet taste via activation of TAS1R/TAS1R2 receptor is of fundamental interest. The difference between hydrogen isotopes is the largest possible isotope effect (doubling of mass in case of deuterium, while tripling in case of tritium), yet deuteration effects on water are generally mild. Nevertheless, water deuteration leads to activation of a GPCR heterodimer to a level that is perceived by humans as sweet taste. While clearly not a practical sweetener, heavy water provides a glimpse into the wide-open chemical space of sweet molecules. Since heavy water may be used in medical procedures, our finding that it can elicit responses of the sweet taste receptor, which is not only located on the tongue but also in other tissues of the human body, represents an important information for clinicians and their patients. Moreover, due to wide application of D₂O in chemical structure determination by NMR, chemists will benefit from being aware of the present observations.

Methods

Sensory evaluation experiments. A human sensory panel was used to resolve the gustatory effect in perception of D₂O taste. Subjects between the ages 20 and 43 years were recruited. The study included 10 experiments with different groups of participants (15–30 subjects; between 4 and 12 males). The perception was tested by sensory tests as detailed below. Either sterile syringes with solutions (0.3 ml) or identical cups with solutions (7 ml), were presented in randomized order, unless otherwise noted. Participants were required to taste each solution using either ‘tip of the tongue’ or ‘sip and spit’ procedures, rinse their mouth with water after each solution and to wait for 30 s before moving to the next taste sample. All research

procedures were ethically approved by the Committee for the Use of Human Subjects in Research in The Robert H. Smith Faculty of Agriculture Food and Environment, the Hebrew University of Jerusalem.

99.9% purity D₂O was purchased from Sigma-Aldrich Corp, while 18 MΩ ultrapure grade was used for pure H₂O. All water samples were placed under vacuum and treated by ultrasound to remove any dissolved gases. See below for more details on water purification.

D-glucose (CAS Number: 50-99-7), sucrose (CAS Number: 57-50-1), cyclamate (CAS Number: 139-05-9), quinine (CAS Number: 207671-44-1), and MSG (CAS Number: 142-47-2) were purchased from Sigma-Aldrich Corp. All compounds were dissolved in both types of water to a final concentration of 50, 75, and 100 mM for D-glucose and sucrose; 3.5, 4.5, and 5.5 mM for cyclamate; 0.1 and 0.32 mM for quinine; 10, 25, and 50 mM for MSG. Lactisole (CAS Number: 150436-68-3) was purchased from Domino Specialty Ingredients and dissolved to a final concentration of 0.9 mM in D₂O water as well as in H₂O. The concentration of lactisole was selected based on previous data^{43,53} and preliminary experiments in our lab, which showed that 0.9 mM decreases the sweetness of 100 mM sucrose. Sweeteners concentrations were selected to be in low intensity of sweetness. All solutions were prepared in the morning of the day of the experiment and were stored in individual plastic syringes (1 ml) for each participant.

The sweetness of heavy water and its effect on other taste compounds was evaluated in several independent experiments: (1) D₂O sweetness relative to H₂O (Fig. 2a); (2) D₂O effect on sweetness of D-glucose (Fig. 2b), sucrose (Fig. 2c), and cyclamate (Fig. 2d); (3) D₂O effect on quinine (Fig. 2e) and MSG (Fig. 2f); (4) Lactisole effect on D₂O sweetness (Fig. 4b); Intensity of each taste modality—sweetness/bitterness/umami was evaluated on a 9-point scale on Compusense Cloud, ranging from 1 (no sensation) to 9 (extremely strong sensation). In addition, participants had to report any additional tastes they recognized. Statistical tests were conducted using JMP Pro 13 (JMP, Version 13. SAS Institute Inc., Cary, NC, 1989–2019).

Data were first analyzed employing ANOVA with participants as a random effect⁵⁴. Thereafter, the Tukey Kramer test was used to compare mean sweetness between all samples⁵⁴. Significance was set at $p < 0.05$, and preplanned comparison *t*-tests were used where relevant.

Details concerning the Two-Alternative Forced Choice test⁵⁵ were as follows: Participants were presented with two blind coded water samples of D₂O and

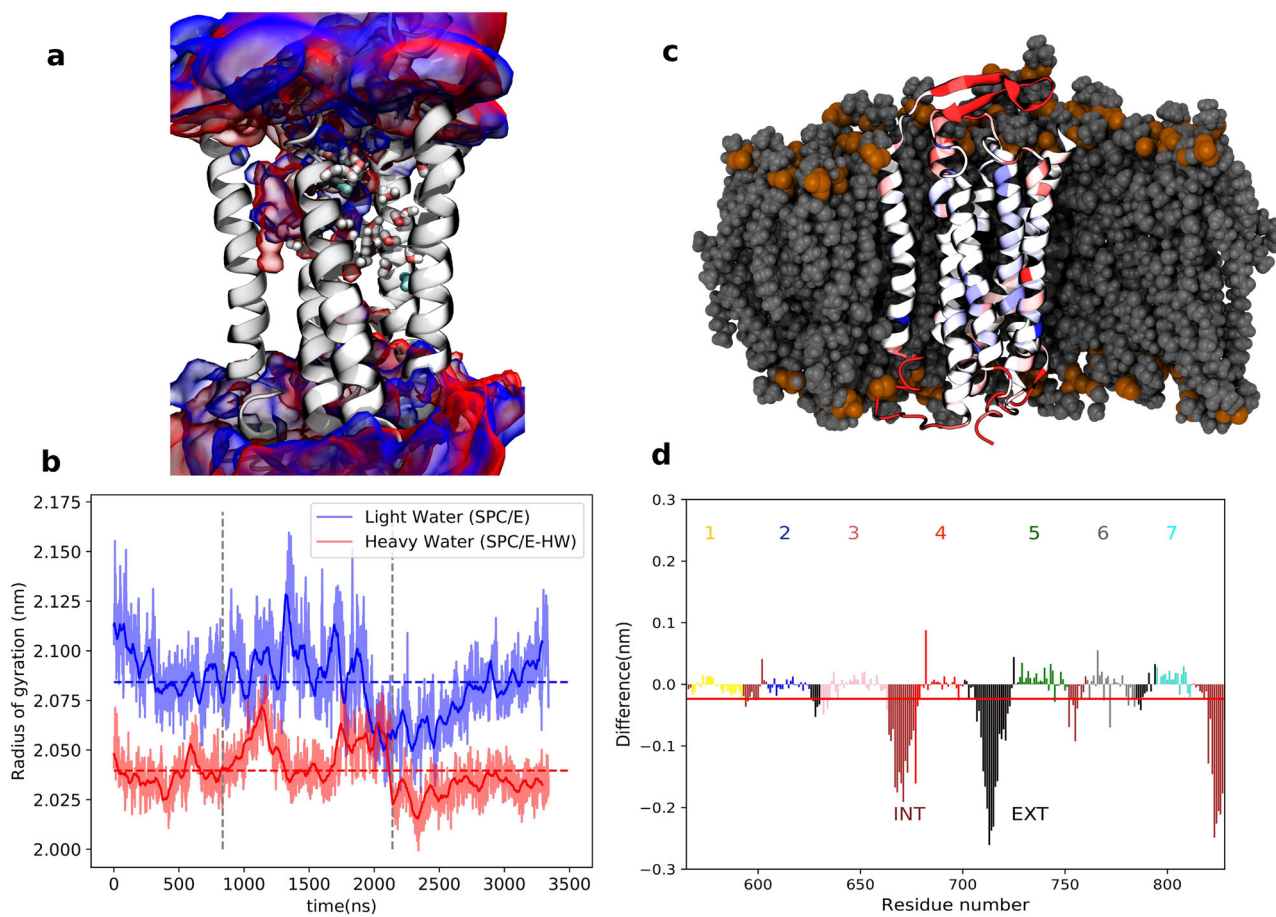


Fig. 7 Differences between the behavior of the transmembrane part of the human sweet taste receptor in H₂O vs D₂O base on analysis of three independent microsecond trajectories. **a** Structure of the TMD of the TAS1R2/TAS1R3 receptor with the probability density (volumetric map) of H₂O (blue) or D₂O (red) molecules within 10 Å from the protein evaluated using the VMD VolMap tool from the MD simulations at an isovalue of 0.1. The conserved water molecules in the X-ray templates are shown in cyan color. Water molecules predicted with the software OpenEye⁵² are shown in licorice representation. **b** Time evolution of the radii of gyration in H₂O (blue) and D₂O (red) from three microsecond-timescale simulations (separated by vertical dashed lines) with total mean values as dashed lines, showing that the protein is more compact in heavy water. **c** Representative snapshot of the transmembrane part of the human sweet taste receptor color-coded that red/blue represents parts more/less rigid in D₂O vs H₂O. The embedding lipid membrane is represented in gray. **d** Difference in root mean square fluctuations in MD trajectories. Negative/positive values mean that structures are more/less rigid in D₂O than in H₂O. The red line represents the sum over all residues. INT intracellular, EXT extracellular.

D₂O + 0.9 mM lactisole. The participants were asked to choose the sweeter solution. For the data analysis, the highest number of responses for one sample was compared to a statistical table⁵⁵ which states the minimum number of responses required for a significant difference.

Panelists were presented with two identical and one different water samples. All three samples were presented to the subjects at once, and the panelists were instructed to taste or smell the samples from left to right and identify the odd sample. Triangle tests were used to examine the difference in taste, as well as in smell, between H₂O and D₂O.

Heterologous expression. TAS1R2/TAS1R3 stimulated activation of the G-protein-mediated pathway was measured applying the IP-One HTRF assay (Cis-bio) based on the manufacturer's protocol. In brief, HEK 293T cells (ATCC) were grown to a confluency of ~85–90% and transiently transfected with 6 µg/plate DNA (TAS1R2, TAS1R3, Gα16gust44) by applying LipofectamineTM 2000 (Invitrogen, USA, 30 µl/plate) transfection reagent, according to the manufacturer's protocol. The next day, cells were suspended with fresh Dulbecco's modified Eagle's medium (DMEM), containing 10% fetal bovine serum (FBS), 1% L-glutamine amino acid and 1% penicillin streptomycin (10% DMEM), seeded (0.5 ml cells per well) into 24-well culture plate, and maintained for 8–12 h at 37 °C. Then cells were "starved" overnight by changing the medium to 0.1% DMEM (containing 0.1% FBS), in order to reduce the basal activity of the cells. Cells exposure was performed by addition of 0.5 ml tested compound (pH = 7.4) dissolved in 0.1% DMEM with 50 mM lithium chloride (LiCl) for 5 min directly into the wells. The presence of LiCl in this step is crucial because LiCl leads to IP1 accumulation⁴⁵. At the end of exposure time, tastant solution was replaced with

fresh medium (0.1% DMEM) containing 50 mM LiCl for another 55 min. Later, wells were washed with 100 µl cold phosphate-buffered saline (PBS) + Triton X-100, and kept at –80 °C for a few hours, in order to dissolve the cell membrane. For the IP-One HTRF assay, cell lysate was mixed with the detection reagents (IP1-d2 conjugate and Anti-IP1 cryptate TB conjugate, each dissolved in lysis buffer), and added to each well in a 384-well plate for 60 min incubation at room temperature. Finally, the plate was read using Clariostar plate reader (BMG, Germany) equipped with 620 ± 10 nm and 670 ± 10 nm filters. IP1 levels were measured by calculating the 665 nm/620 nm emission ratio.

All responses are presented as the means ± SEM of IP1 accumulation (%). Dose–response curves were fitted by non-linear regression using the algorithms of PRISM 7 (GraphPad Software, San Diego, CA, USA). Column figures were analyzed using one-way ANOVA with a Dunnett's⁵⁴. Each compound was tested in triplicate in three individual experiments in comparison to the reference (carbachol dissolved in H₂O or basal levels)⁴⁵.

In the case of D₂O, in order to test its specific effect, we used a powder DMEM medium (CAS Number: D5030, Sigma-Aldrich), dissolved in the needed amount of D₂O instead of the liquid one. Other ligands than D₂O were purchased from Sigma-Aldrich or Domino Specialty Ingredients as noted above. Unless noted otherwise, ligands were used at final concentrations of 5, 50, 480, 960, 1.8 × 10³, and 2.1 × 10³ mM for D-glucose; 0.1, 1, and 15 mM for carbachol and D₂O at 0–100% proportionately to H₂O. Since there was no prior literature on concentrations of lactisole for this assay, the value of 2 mM was chosen based on preliminary experiment with several lactisole concentrations and their effect on IP1 values due to exposure to D-glucose.

For the functional assays with the human sweet taste receptor, we used a cell line (HEK 293 FlpIn T-Rex), which constitutively expresses the sweet taste receptor

subunit TAS1R2 as well as the chimeric G protein Ga15gi3, whereas the sweet taste receptor subunit TAS1R3 can be induced by tetracycline^{43,44}. Gai3 is one of the major species of G α -subunits capable of coupling to taste receptors, along with G α -gustducin, G α S, and Gai2^{56,57} and TAS1R2-TAS1R3-Gai3 cell system was successfully used in a previous study⁴³. The functional experiments were done as described before⁴⁴. Briefly, the cells were grown in DMEM supplemented with 10% fetal bovine serum, 100 U Penicillin/ml, 0.1 mg/ml Streptomycin, 2 mM L-glutamine, at 37 °C and 5%-CO₂, 100% air humidity. The day before the experiment, cells were seeded to a density of 50–60% onto 96-well plates coated with 10 μ g/ml poly-D-lysine and 0.5 μ g/ml tetracycline was added. Next, cells were loaded with Fluo-4 AM in the presence of 2.5 mM probenecid for 1 h. After this, cells were washed twice with C1-buffer (130 mM NaCl, 5 mM KCl, 10 mM HEPES, 1 mM sodium pyruvate, and 2 mM CaCl₂, pH 7.4) before placing them in a fluorometric imaging plate reader (FLIPR^{tera}, Molecular Devices) for measurements.

C1-buffer prepared with D₂O was mixed with C1-buffer made with H₂O to result in the following final D₂O-concentrations (a further threefold dilution, which occurs upon application of 50 μ L stimulus to 100 μ L of C1-buffer in the 96-well plates is already included): 18.47, 5.84, 1.85, 0.584, 0.185, 0.058, 0.018, and 0.000 M. Fluorescence changes were monitored after automated application of stimuli. As specificity control C1-D₂O including 0.9 mM lactisole, a selective inhibitor of the human sweet taste receptor⁵⁸, was applied to identically treated cells. This concentration is the same as used in sensory experiments and close to the 1 mM used in calcium assays in previous work⁴³. Experimental results from five biological replicates performed in quadruplicates were used to establish the dose–response relationship using the software SigmaPlot as before⁴⁴. As the highest D₂O-concentration resulted in fluorescence changes largely resistant to lactisole blocking, the 18.47 M concentration was excluded. Student's *t*-test was used to confirm that D₂O-induced fluorescence changes above baseline were significantly ($p \leq 0.01$) different from lactisole-treated controls.

Animal experiments. All animal experiments followed the ethical guidelines for animal experiments and the Act of the Czech Republic Nr. 246/1992 and were approved by the Committee for Experiments with Laboratory Animals of the Czech Academy of Sciences. Three-month-old male C57BL/6J mice ($n = 34$) from Charles Rivers Laboratories (Sulzfeld, Germany) were housed at a temperature of 23 °C with a daily cycle of 12 h light and dark (lights on at 6 am). The mice were placed in groups of two in cages with automatic drinking monitoring system (Developmental Workshops of Institute of Organic Chemistry and Biochemistry of the Czech Academy of Sciences, Prague, Czech Republic). They were given ad libitum water and a standard rodent chow diet (Sniff Spezialdiäten GmbH, Soest, Germany). On the day of the experiment, during the dark phase of the cycle, freely fed mice were given weighed food pellets and two 30 ml glass bottles. The two bottles contained pure H₂O and pure D₂O ($n = 12$), or H₂O and sucrose solution (43 mmol/l sucrose solution in H₂O) ($n = 10$), see Table S1. Mice drinking H₂O in both bottles served as a control group ($n = 12$). Drinking was monitored every 10 min for 16 h (starting from 6 pm) and food intake was determined at the end of the experiment (Figure S5).

All responses are presented as the means \pm SEM. Statistical analysis was performed using ANOVA with a Dunnett's test⁵⁴ for food intake. Two-way ANOVA with a Bonferroni's multiple comparisons test was used for analysis of average volume of liquid consumption. Analysis was performed using GraphPad Software, Inc., Prism 8 (GraphPad Software, San Diego, CA, USA). The differences between the control and treated groups were considered significant at $p < 0.05$.

Modeling and docking. All models were prepared with I-Tasser web server⁵¹. The templates that were used by I-Tasser for each of the TAS1R2 and TAS1R3 monomers were: 6N51, 5X2M, and 5K5S. To model the full heterodimer, the monomer models were aligned to a Class-C GPCR Cryo-EM structure (PDB: 6N51) and minimized with Schrödinger Maestro 2019-1. To illustrate the orthosteric binding site of sugars D-glucose was prepared (Schrödinger Maestro 2019-1, LigPrep) and docked with Glide XP, to the TAS1R2 VFT domain model that was based on 5X2M in a protocol that was validated in previous work⁵⁹. The TAS1R3-binding site is based on a lactisole molecule docked to TAS1R3 TMD model (Schrödinger Maestro 2018-2, Glide SP, template PDB ID: 4OR2 and 4OO9). The figure was made using ChimeraX (version 0.93)⁶⁰. Water molecules were predicted with a water mapping software (SZMAP 1.5.0.2: OpenEye⁵²) after a successful benchmark over conserved water templates (PDB IDs 5CGC and 5CGD), in which the software was able to identify overall 8 out of 10 crystal water molecules around the ligands of the templates.

Reporting summary. Further information on research design is available in the Nature Research Reporting Summary linked to this article.

Data availability

The data sets generated during the current study are available as Supplementary Data.

Received: 12 August 2020; Accepted: 25 February 2021;

Published online: 06 April 2021

References

- Urey, H. C., Brickwedde, F. G. & Murphy, G. M. A hydrogen isotope of mass 2. *Phys. Rev.* **39**, 164–165 (1932).
- Francl, M. The weight of water. *Nat. Chem.* **11**, 284–285 (2019).
- Clark, T., Heske, J. & Kühne, T. D. Opposing electronic and nuclear quantum effects on hydrogen bonds in H₂O and D₂O. *ChemPhysChem* **20**, 2461–2465 (2019).
- Paesani, F. & Voth, G. A. The properties of water: insights from quantum simulations. *J. Phys. Chem. B* **113**, 5702–5719 (2009).
- Macdonald, F. & Lide, D. R. CRC handbook of chemistry and physics: from paper to web. *Abstr. Pap. Am. Chem. Soc.* **225**, U552–U552 (2003).
- Bogan, R. A. J., Ohde, S., Arakaki, T., Mori, I. & McLeod, C. W. Changes in rainwater pH associated with increasing atmospheric carbon dioxide after the industrial revolution. *Water, Air, Soil Pollut.* **196**, 263–271 (2009).
- Van Horn, E. & Ware, G. C. Growth of bacterium coli and staphylococcus albus in heavy water. *Nature* **184**, 833–833 (1959).
- Mosin, O., Ignatov, I., Skladnev, D. & Shvets, V. Studying of phenomenon of biological adaptation to heavy water. *Eur. J. Mol. Biotechnol.* **6**, 180–209 (2014).
- Kampmeyer, C. et al. Mutations in a single signaling pathway allow cell growth in heavy water. *ACS Synth. Biol.* **9**, 733–748 (2020).
- Barbour, H. G. The basis of the pharmacological action of heavy water in mammals. *Yale J. Biol. Med.* **9**, 551–565 (1937).
- Czajka, D. M., Finkel, A. J., Fischer, C. S. & Katz, J. J. Physiological effects of deuterium on dogs. *Am. J. Physiol.-Leg. Content* **201**, 357–362 (1961).
- Dansgaard, W. Stable isotopes in precipitation. *Tellus* **16**, 436–468 (1964).
- Jones, P. J. H. & Leatherdale, S. T. Stable isotopes in clinical research: safety reaffirmed. *Clin. Sci.* **80**, 277–280 (1991).
- Speakman, J. & Speakman, J. R. The history and theory of the doubly labeled water technique. *Am. J. Clin. Nutr.* **68**, 932S–938S (1998).
- Pittendrigh, C. S., Caldarola, P. C. & Cosbery, E. S. A differential effect of heavy water on temperature-dependent and temperature-compensated aspects of the circadian system of *Drosophila pseudoobscura*. *Proc. Natl Acad. Sci. USA* **70**, 2037 (1973).
- Richter, C. P. Heavy water as a tool for study of the forces that control length of period of the 24-hour clock of the hamster. *Proc. Natl Acad. Sci. USA* **74**, 1295–1299 (1977).
- Hansen, K. & Rustung, E. Untersuchen über die Biologische Wirkungen von "Schwerem Wasser" bei Warmblütigen Tieren. *Klinische Wochenschr.* **14**, 104–108 (1935).
- Urey, H. C. & Failla, G. Concerning the taste of heavy water. *Science* **81**, 273 (1935).
- Kirby, R. H., Pick, D. F. & Riddick, M. S. Discrimination between heavy water and deionized water using gustation vs. olfaction in humans. *Physiological Psychol.* **4**, 102–104 (1976).
- Richter, C. P. Study of taste and smell of heavy-water (99.8percent) in rats. *Proc. Soc. Exp. Biol. Med.* **152**, 677–684 (1976).
- Miller, I. J. & Mooser, G. Taste responses to deuterium-oxide. *Physiol. Behav.* **23**, 69–74 (1979).
- Nelson, G. et al. Mammalian sweet taste receptors. *Cell* **106**, 381–390 (2001).
- Li, X. et al. Human receptors for sweet and umami taste. *Proc. Natl Acad. Sci. USA* **99**, 4692 (2002).
- Di Pizio, A. & Niv, M. Y. Computational studies of smell and taste receptors. *Isr. J. Chem.* **54**, 1205–1218 (2014).
- Gutierrez, R., Fonseca, E. & Simon, S. A. The neuroscience of sugars in taste, gut-reward, feeding circuits, and obesity. *Cell. Mol. Life Sci.* **77**, 3469–3502 (2020).
- Damak, S. et al. Detection of sweet and umami taste in the absence of taste receptor T1r3. *Science* **301**, 850–853 (2003).
- Yee, K. K., Sukumaran, S. K., Kotha, R., Gilbertson, T. A. & Margolskee, R. F. Glucose transporters and ATP-gated K⁺ (KATP) metabolic sensors are present in type I taste receptor 3 (T1r3)-expressing taste cells. *Proc. Natl Acad. Sci. USA* **108**, 5431–5436 (2011).
- Bachmanov, A. A., Tordoff, M. G. & Beauchamp, G. K. Sweetener preference of C57BL/6ByJ and 129P3/J mice. *Chem. Senses* **26**, 905–913 (2001).
- Jiang, P. et al. Identification of the cyclamate interaction site within the transmembrane domain of the human sweet taste receptor subunit T1R3. *J. Biol. Chem.* **280**, 34296–34305 (2005).
- Jiang, P. et al. Lactisole interacts with the transmembrane domains of human T1R3 to inhibit sweet taste. *J. Biol. Chem.* **280**, 15238–15246 (2005).
- Zhao, G. Q. et al. The receptors for mammalian sweet and umami taste. *Cell* **115**, 255–266 (2003).

32. Chaudhari, N. & Roper, S. D. The cell biology of taste. *J. cell Biol.* **190**, 285–296 (2010).
33. Dagan-Wiener, A. et al. BitterDB: taste ligands and receptors database in 2019. *Nucleic Acids Res.* **47**, D1179–D1185 (2019).
34. Dagan-Wiener, A. et al. Bitter or not? BitterPredict, a tool for predicting taste from chemical structure. *Sci. Rep.* **7**, 12074 (2017).
35. Cioni, P. & Strambini, G. B. Effect of heavy water on protein flexibility. *Biophysical J.* **82**, 3246–3253 (2002).
36. Gane, S. et al. Molecular vibration-sensing component in human olfaction. *PLoS ONE* **8**, e55780 (2013).
37. Block, E., Jang, S., Matsunami, H., Batista, V. S. & Zhuang, H. Reply to Turin et al.: Vibrational theory of olfaction is implausible. *Proc. Natl Acad. Sci.* **112**, E3155 (2015).
38. Vosshall, L. B. Laying a controversial smell theory to rest. *Proc. Natl Acad. Sci. USA* **112**, 6525 (2015).
39. Low, J. Y. Q., McBride, R. L., Lacy, K. E. & Keast, R. S. J. Psychophysical evaluation of sweetness functions across multiple sweeteners. *Chem. Senses* **42**, 111–120 (2017).
40. Mennella, J. A., Reed, D. R., Mathew, P. S., Roberts, K. M. & Mansfield, C. J. “A spoonful of sugar helps the medicine go down”: bitter masking by sucrose among children and adults. *Chem. Senses* **40**, 17–25 (2014).
41. Ben Abu, N., Harries, D., Voet, H. & Niv, M. Y. The taste of KCl—What a difference a sugar makes. *Food Chem.* **255**, 165–173 (2018).
42. Dubovski, N., Ert, E. & Niv, M. Bitter mouth-rinse affects emotions. *Food Quality. Prefer.* **60**, 154–164 (2017).
43. Galindo-Cuspinera, V., Winnig, M., Bufer, B., Meyerhof, W. & Breslin, P. A. S. A TAS1R receptor-based explanation of sweet ‘water-taste’. *Nature* **441**, 354–357 (2006).
44. Behrens, M., Blank, K. & Meyerhof, W. Blends of non-caloric sweeteners saccharin and cyclamate show reduced off-taste due to TAS2R bitter receptor inhibition. *Cell Chem. Biol.* **24**, 1199–119 (2017).
45. Trinquet, E. et al. d-myo-Inositol 1-phosphate as a surrogate of d-myo-inositol 1,4,5-tris phosphate to monitor G protein-coupled receptor activation. *Anal. Biochem.* **358**, 126–135 (2006).
46. Zhang, R. & Xie, X. Tools for GPCR drug discovery. *Acta Pharmacol. Sin.* **33**, 372–384 (2012).
47. Hussmann, G. P., Yasuda, R. P., Xiao, Y., Wolfe, B. B. & Kellar, K. J. Endogenously expressed muscarinic receptors in HEK293 cells augment up-regulation of stably expressed $\alpha 4\beta 2$ nicotinic receptors. *J. Biol. Chem.* **286**, 39726–39737 (2011).
48. Ueda, T., Ugawa, S., Yamamura, H., Imaizumi, Y. & Shimada, S. Functional interaction between T2R taste receptors and G-protein alpha subunits expressed in taste receptor cells. *J. Neurosci.* **23**, 7376–7380 (2003).
49. Mason, J. S., Bortolato, A., Congreve, M. & Marshall, F. H. New insights from structural biology into the druggability of G protein-coupled receptors. *Trends Pharmacol. Sci.* **33**, 249–260 (2012).
50. Venkatakrishnan, A. J. et al. Diverse GPCRs exhibit conserved water networks for stabilization and activation. *Proc. Natl Acad. Sci. USA* **116**, 3288–3293 (2019).
51. Yang, J. & Zhang, Y. I-TASSER server: new development for protein structure and function predictions. *Nucleic Acids Res.* **43**, W174–W181 (2015).
52. Bayden, A. S., Moustakas, D. T., Joseph-McCarthy, D. & Lamb, M. L. Evaluating free energies of binding and conservation of crystallographic waters using SZMAP. *J. Chem. Inf. Modeling* **55**, 1552–1565 (2015).
53. Galindo-Cuspinera, V. & Breslin, P. A. S. The liaison of sweet and savory. *Chem. Senses* **31**, 221–225 (2005).
54. Sutton, S. Encyclopedia of research design. *Libr. J.* **135**, 105–106 (2010).
55. Kemp, S. E., Hollowood, T. & Hort, J. *Sensory Evaluation: A Practical Handbook* xi, 196p (Ames Wiley-Blackwell, 2009).
56. McLaughlin, S. K., McKinnon, P. J., Spickofsky, N., Danho, W. & Margolskee, R. F. Molecular-cloning of G-proteins and phosphodiesterases from rat taste cells. *Physiol. Behav.* **56**, 1157–1164 (1994).
57. Kusakabe, Y. et al. Comprehensive study on G protein alpha-subunits in taste bud cells, with special reference to the occurrence of G alpha i2 as a major G alpha species. *Chem. Senses* **25**, 525–531 (2000).
58. Sclafani, A. & Perez, C. Cypha(TM) propionic acid, 2-(4-methoxyphenol) salt inhibits sweet taste in humans, but not in rats. *Physiol. Behav.* **61**, 25–29 (1997).
59. Ben Shoshan-Galeczki, Y. & Niv, M. Y. Structure-based screening for discovery of sweet compounds. *Food Chem.* **315**, 126286 (2020).
60. Goddard, T. D. et al. UCSF ChimeraX: meeting modern challenges in visualization and analysis. *Protein Sci.* **27**, 14–25 (2018).

Acknowledgements

We thank R.F. Margolskee for the pcDNA of chimeric Ga16gust44 and P. Jiang and Y. Wang for hosting N.B.A. in Monell Chemical Senses Center during preliminary stages of this project. V.P. and L.M. acknowledge Ondřej Pačes and his team for the development of automatic drinking monitoring system, and Hedvika Vysušilová for outstanding technical assistance and animal handling. M.B. thanks Catherine Delaporte for excellent technical assistance. P.J. thanks the Czech Science Foundation for support via an EXPRO grant no. 19-26854X. V.C.C. and C.T. acknowledge support from the Charles University in Prague and from the International Max Planck Research School in Dresden. Funding by ISF grant #1129/19 and UHJ-France and the Foundation Scopos to M.Y.N. is gratefully acknowledged. M.Y.N. is a member of COST actions Mu.Ta.Lig (CA15135) and ERNEST (CA18133). P.E.M. acknowledges support from the viewers of his YouTube popular science channel.

Author contributions

N.B.A., P.E.M., M.Y.N., and P.J. designed the study, N.B.A. and H.K. performed sensory experiments, N.B.A. and E.M. carried out IP1 experiments, M.B. conducted calcium imaging experiments, N.D. and Y.B.S.G. performed homology modeling and structural analyses, P.E.M. performed water purification, J.C. performed water purity tests, V.P. and L.M. performed experiments on mice, V.C.C. developed the heavy water interaction potential, and C.T. performed the molecular dynamics simulations. P.J., M.Y.N., and N.B.A. wrote the paper with input from all co-authors.

Competing interests

The authors declare no competing interests.

Additional information

Supplementary information The online version contains supplementary material available at <https://doi.org/10.1038/s42003-021-01964-y>.

Correspondence and requests for materials should be addressed to M.Y.N. or P.J.

Reprints and permission information is available at <http://www.nature.com/reprints>

Publisher's note Springer Nature remains neutral with regard to jurisdictional claims in published maps and institutional affiliations.



Open Access This article is licensed under a Creative Commons Attribution 4.0 International License, which permits use, sharing, adaptation, distribution and reproduction in any medium or format, as long as you give appropriate credit to the original author(s) and the source, provide a link to the Creative Commons license, and indicate if changes were made. The images or other third party material in this article are included in the article's Creative Commons license, unless indicated otherwise in a credit line to the material. If material is not included in the article's Creative Commons license and your intended use is not permitted by statutory regulation or exceeds the permitted use, you will need to obtain permission directly from the copyright holder. To view a copy of this license, visit <http://creativecommons.org/licenses/by/4.0/>.

© The Author(s) 2021